Downstream Amplification and Formation of Monsoon Disturbances

T. N. KRISHNAMURTI, JOHN MOLINARI, HUA-LU PAN AND VINCE WONG

Department of Meteorology, Florida State University, Tallahassee 32306

(Manuscript received 25 April 1977, in revised form 21 June 1977)

ABSTRACT

In this paper we present many examples (based on 43 years of data) of a phenomenon of downstream amplification over the monsoonal belt. The specific finding here is the following sequence of events: 1) During northern summer pressure drops in the vicinity of the North Vietnam coast (near 20°N) as a typhoon or a tropical storm arrives; 2) during the ensuing week pressure rises over Indochina and Burma by some 5–7 mb; and 3) during the following week a monsoon disturbance forms near the northern part of the Bay of Bengal. On an x-t (or Hovmöller) diagram this sequence of low-high-low formation is similar to the downstream amplification phenomenon of the middle latitudes. The following are some interesting differences: over the middle latitudes the eastward propagating phase velocity is of the order of 10° longitude day^{-1}, while the eastward propagating group velocity (the speed of propagation of the amplification) is around 30° longitude day^{-1}. The tropical counterparts are westward propagating, and the phase and group velocity are, respectively, around 6° and 2° longitude day^{-1}. In meteorological literature one frequently notes reference to *in situ* formation of monsoon depressions over the northern part of the Bay of Bengal. Our study illustrates the superposition of stationary long waves with progressive short waves, the latter arriving from the western Pacific. This result is contrary to this notion of *in situ* formation. In this paper we examine some aspects of this slowly westward propagating group velocity phenomenon.

1. Introduction

In this paper we are interested in portraying a mechanism for the formation of monsoon disturbances (monsoon lows and depressions) over the Bay of Bengal. During Northern Hemisphere summer, a number of monsoon disturbances are known to form over the northern part of the Bay of Bengal. Fig. 1 illustrates the tracks of a number of monsoon disturbances based on 70 years of observations for the month of July (India Meteorological Department, 1964). Since all of the tracks originate in the Bay of Bengal, the notion that they form *in situ* over the water has prevailed in the meteorological literature. Keshavamurty (1971) has emphasized the importance of barotropic instability during the formative stages of the monsoon disturbances. He has also suggested that the role of convection is perhaps only important in the subsequent stages of development of the depression. The possible importance of the combined barotropic-baroclinic instability mechanism has also been suggested by various authors. Lack of adequate upper air observations has limited any definitive analysis of the initial formation of these disturbances. Their structure has been illustrated in a number of observational studies (Krishnamurti *et al.*, 1975; Murakami, 1976), which will not be reviewed here.

Photographs from polar orbiting satellites do not usually exhibit westward propagating cloud clusters that move from the western Pacific across Indochina, Burma and into the northern part of the Bay of Bengal (Wallace, 1970). This has tended to confirm the notion of an *in situ* formation of Bay of Bengal disturbances.

Our investigations of westward propagating wave disturbances lead us to take exception to this notion of *in situ* formation. This paper is aimed at showing that scale interactions of westward moving wavetrains give rise to a westward propagating downstream amplification. A teleconnection between western Pacific disturbances and Bay of Bengal disturbances is illustrated from 43 years of surface pressure data records. Our study emphasizes the importance of the following sequence of events from several examples of the formation of Bay of Bengal disturbances:

1) A western Pacific typhoon or tropical storm arrives and/or begins to recurve over the Asian coast near 20°N.

2) The lowering of surface pressure over southern China and Vietnam is followed by a gradual rise of pressure further inland over Indochina and Burma for roughly a one-week period. The amplitude of the pressure rise is on the order of 5 mb.

3) A lowering of pressure and the formation of a monsoon disturbance occurs over the Bay of Bengal during the following four or five days.

The phenomenon can be best illustrated on a trough-ridge or Hovmöller diagram (Hovmöller, 1949), which

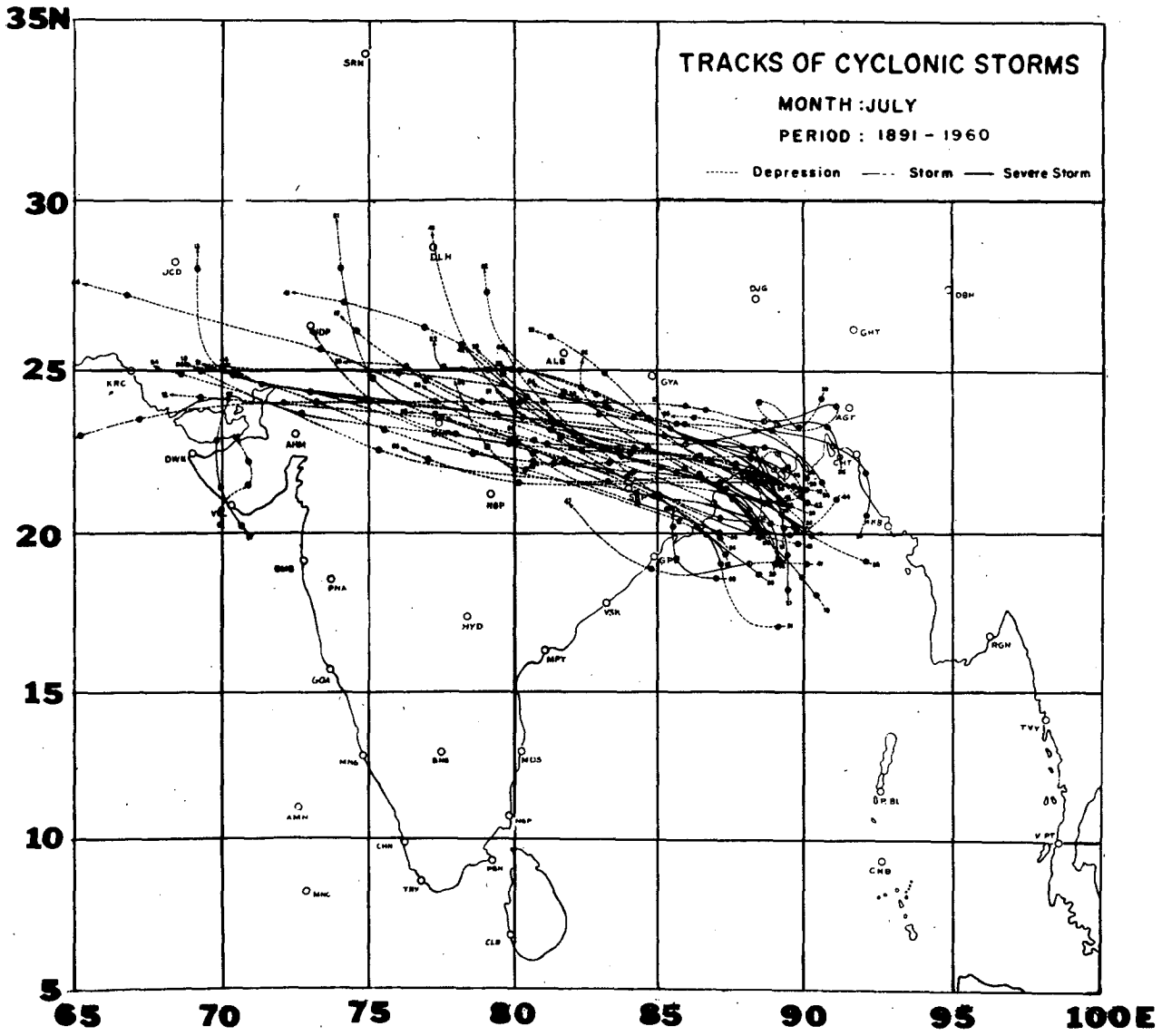

FIG. 1. The tracks of a number of monsoon disturbances during July for a 70-year period from 1891–1960 (India Meteorological Department, 1964).

clearly shows the downstream amplification and a teleconnection with the western Pacific disturbance. The amplification is "downstream" in the sense that the tropospheric mean zonal velocity is from the east. In the rest of this paper we shall analyze this phenomenon and portray its similarity to mid-latitude events of downstream amplification of upper troughs. We should at the beginning emphasize that the mechanism suggested here is not an all inclusive one. However, 35 well-defined examples have been found, suggesting that downstream amplification is an important mechanism in the formation of monsoon disturbances.

2. Downstream amplification in middle latitudes

The Hovmöller diagram has been widely used in middle latitudes. Fig. 2 is a typical example of downstream amplification based on 700 mb geopotential height charts. This downstream amplification of trought and ridges in middle latitudes is known to propagate as a speed of roughly 30° longitude day^{-1} eastward. This speed is usually identified with the group velocity of Rossby waves whose phase speeds are about one-third this value. The synoptic sequence of events that often occurs is the following: In the Northern Hemisphere winter season, along 33°N, a major upper trough forms off the coast of Japan. A long-wave ridge intensifies a few days thereafter over the mid-Pacific ocean. This is followed by intensification of a trough off the coast of California several days later. Diagrams illustrating such amplification have appeared in the meteorological literature for both Northern and Southern Hemisphere weather events. Krishnamurti and Higgins (1967)

showed that the downstream intensification is usually accompanied by a large local increase of vorticity in the developing upper troughs. Thus we cannot regard this as a purely barotropic group velocity phenomenon. This downstream amplification can be viewed as a teleconnection between the occurrences in two separated regions, and is somewhat simpler to understand than other teleconnections that have usually been mentioned as remote phenomenological associations.

Although the essential geometry of the middle-latitude 500 mb heights on a Hovmöller diagram appears similar in most of the downstream amplification situations, the precise location where the successive troughs and ridges amplify depends much on the prevailing long-wave positions. Such an impulse is at times associated with the development of an upper ridge over North America and at other times with the deepening of an upper trough over the same region. Because of differences in wavelengths and locations from one situation to another, it is not practical to produce, for middle latitudes, a composite illustration of such events. Instead, we shall describe briefly the wave superpositions that occurred in a typical mid-latitude event. Later we shall present tropical illustrations of such a phenomenon and show the degree of similarity between the low- and high-latitude wave interactions.

Fig. 3a illustrates a downstream amplification event at 500 mb during February 1962 over the Pacific Ocean at 35°N. The trough develops at 160°E on about 9 February, followed by a middle Pacific ridge buildup and a deepening of the trough off the coast of California. A zonal harmonic analysis of the 500 mb height data shows that this geometry is a superposition of 1) rapidly eastward moving long waves (Fig. 3b), i.e., wavenumbers 1, 2, and 3 and, 2) slowly eastward moving shorter waves (Fig. 3c), i.e., wavenumbers 4, 5 and 6. Fig. 3d illustrates the sum of the first six zonal harmonics which carry roughly 80% of the total variance shown in Fig. 3a. The essential phenomenon is described by the first six zonal harmonics. The manner in which the downstream amplification results from wave superposition is as follows. The shorter waves

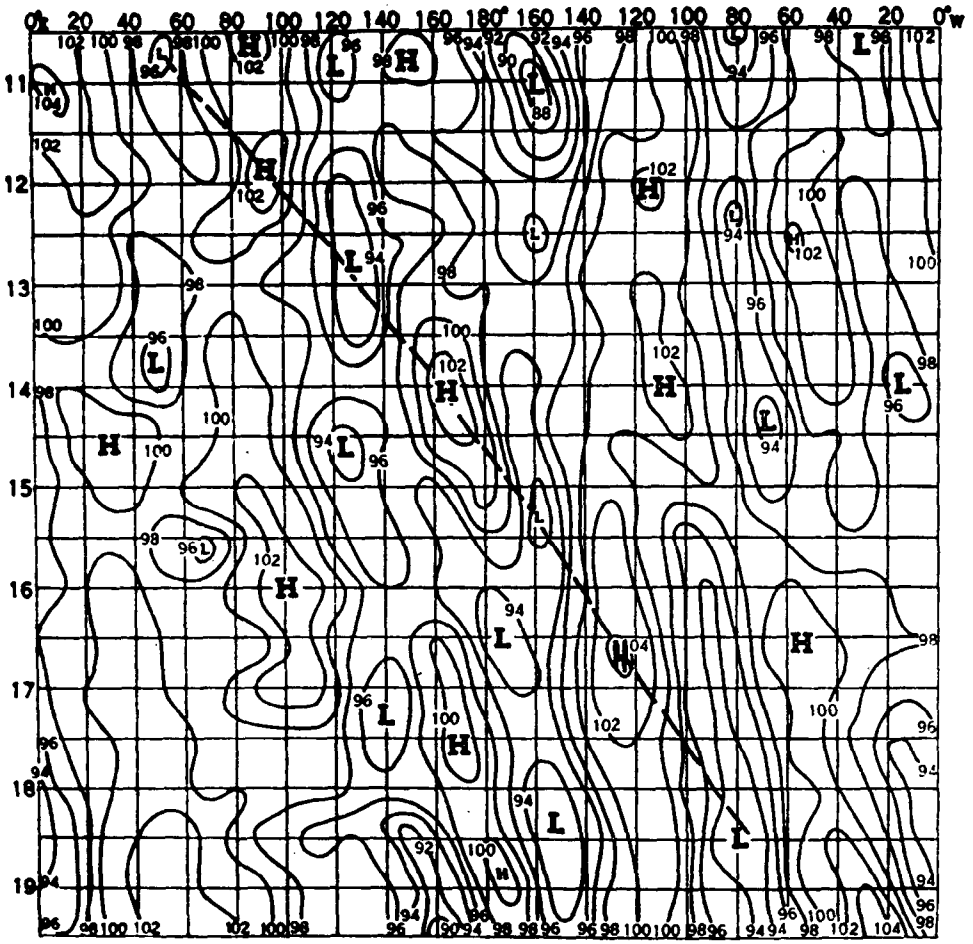

FIG. 2. Trough-ridge diagram at 50°N (700 mb). Time is along ordinate, 11 to 19 October 1948. Longitude is along abscissa. The 700 mb heights are in hundreds of feet. (Diagram based on Parry and Roe, 1952.)

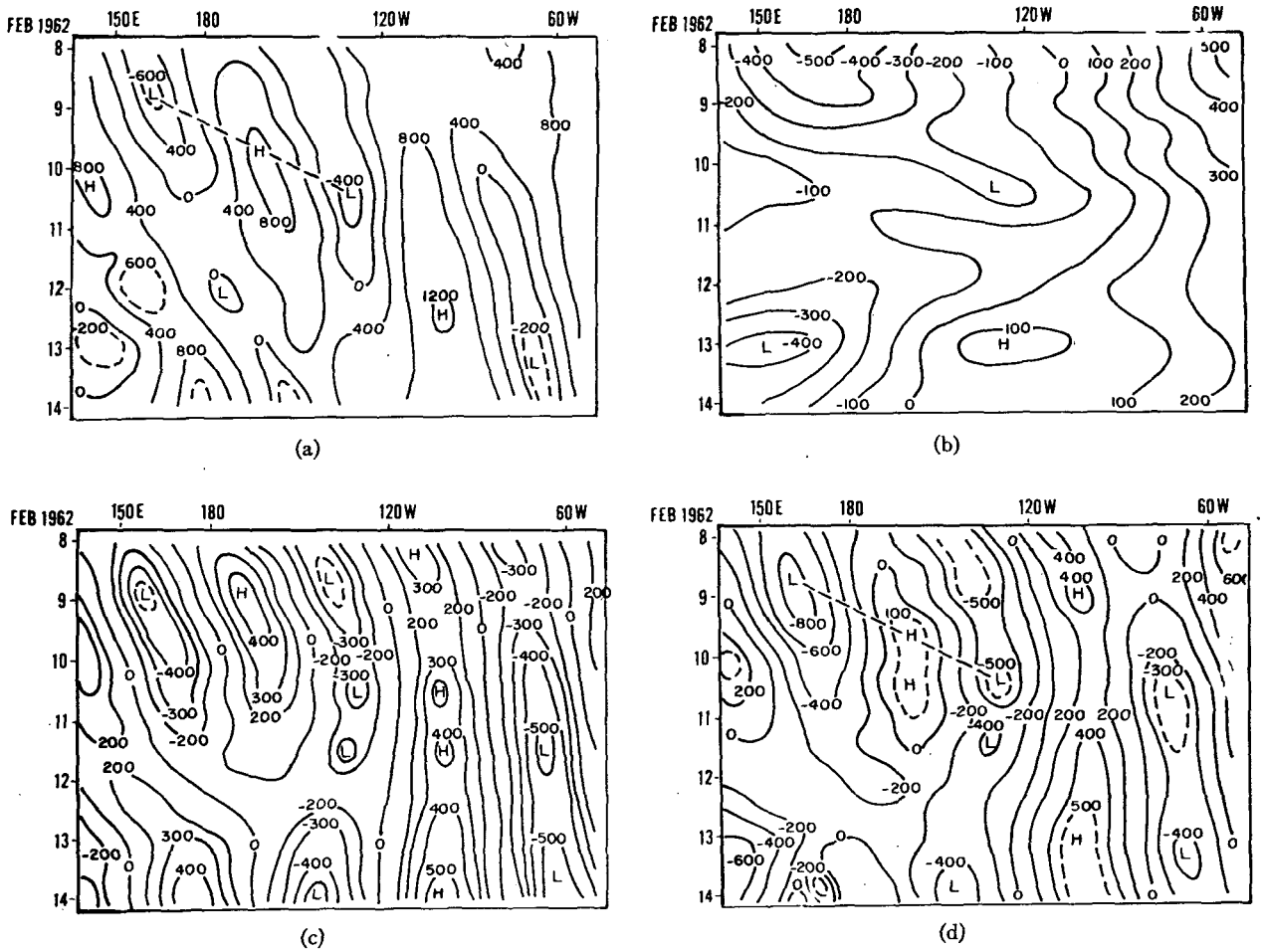

FIG. 3. Hovmöller diagrams at 35°N during February 1962 at 500 mb for (a) sum of all wavenumbers; (b) sum of zonal wavenumbers 1, 2 and 3; (c) sum of zonal wavenumbers 4, 5 and 6; and (d) sum of zonal wavenumbers 1–6. Values are in feet.

alone (wavenumbers 4, 5 and 6) do not exhibit a downstream amplification (see Fig. 3c). In fact, these waves show a trough off the coast of Japan, a mid-Pacific ridge and a trough off the California coast at the initial stage which gradually propagate eastward and weaken somewhat. The long waves alone also do not display the downstream amplification phenomenon. Fig. 3b shows a slow eastward progression and a subsequent westward motion for the long waves. In this diagram a characteristic feature is the large amplitude of the long waves during the initial stages. The amplitude of the long waves decreases considerably during the eastward propagation of the downstream amplification. This feature, as we shall show later, also occurs during the westward propagation of the tropical counterpart. This large change in the long-wave amplitude from 500 to 100 units suggests that the phenomenon cannot be viewed as a simple linear Rossby wave superposition. Although, in principle, linear superposition of two or more waves can describe the propagation of a downstream amplification, atmospheric observations, such as those presented here, seem somewhat more complex and we feel that linear superposition exercises have only a limited scope.

3. Examples of downstream amplification for the monsoons

Fig. 4 gives a number of examples of the teleconnection between western Pacific typhoons and monsoon disturbances. The left panel shows the departure of the surface pressure from 1000 mb during a selected 21-day period centered on a date when the Pacific ridge was building over Indochina. The right panel illustrates the track of the typhoon (or tropical storm) for each case and its central pressure at 0000 GMT.

The existence of the phenomenon of downstream amplification is very clearly demonstrated by these Hovmöller diagrams. Forty-three years (1933–76) of once-daily surface pressure records from the archives of the National Center for Atmospheric Research were examined in this study. No data were available for 1945. The surface pressure data were used in their original form without any smoothing.

Thirty-five examples of downstream amplification

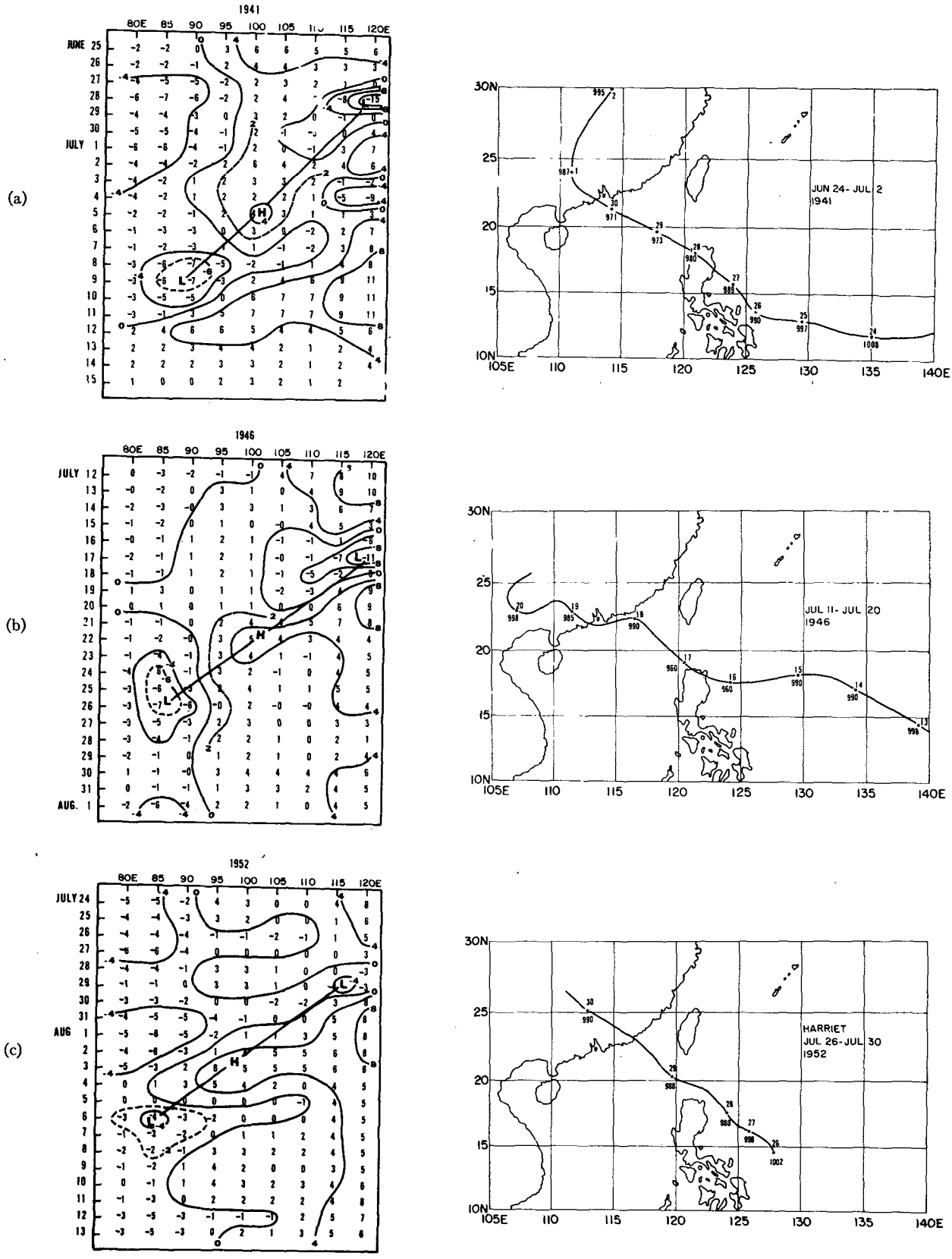

FIG. 4. (Left panel) Hovmöller diagrams of surface pressure data at 20°N. The ordinate shows the date and the abscissa longitude. The surface pressures are departures from 1000 mb. (Right panel) Typhoon tracks for the downstream amplification illustrated in the left panel. Central pressures at 0000 GMT are shown, when available. (Sources: Central Meteorological Observatory, Tokyo, 1951; Chin, 1958; U.S. Fleet Weather Central, 1960–1975.)

(d)

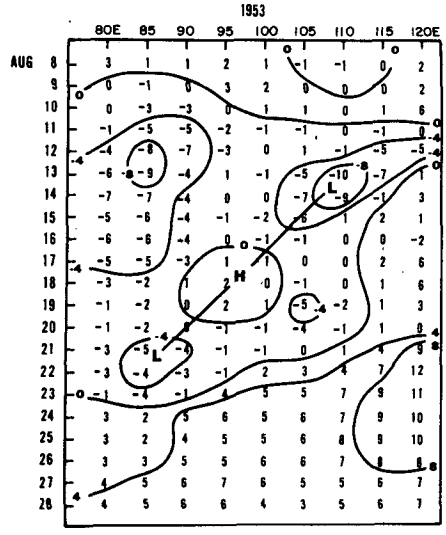

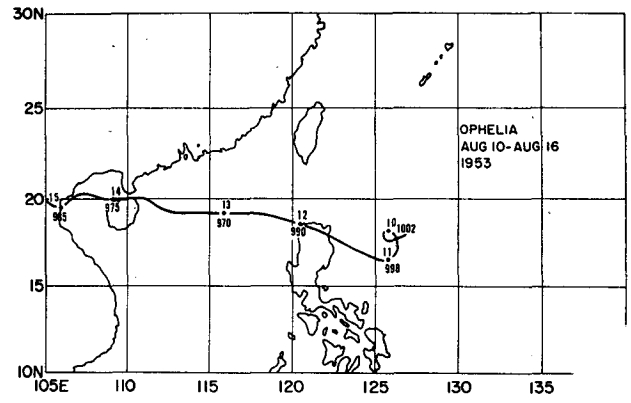

(e)

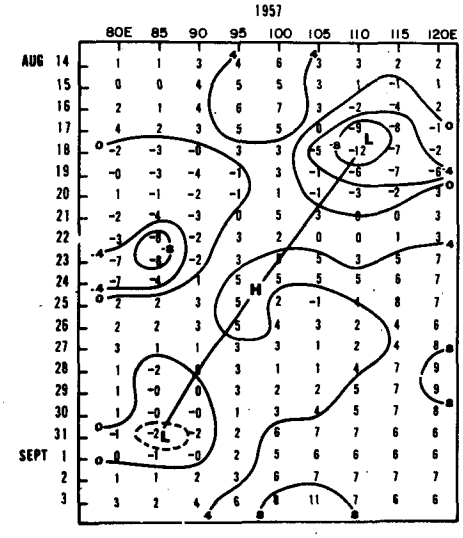

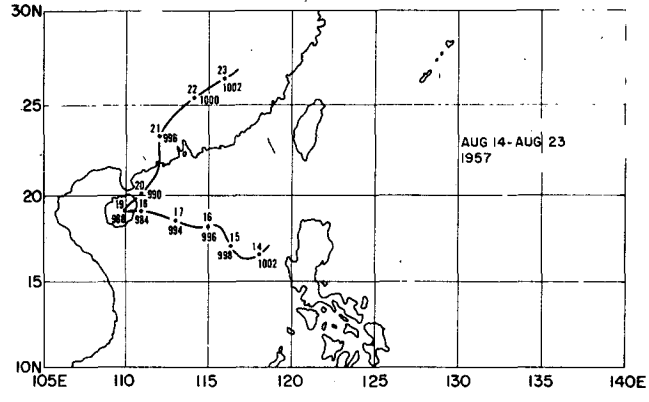

(f)

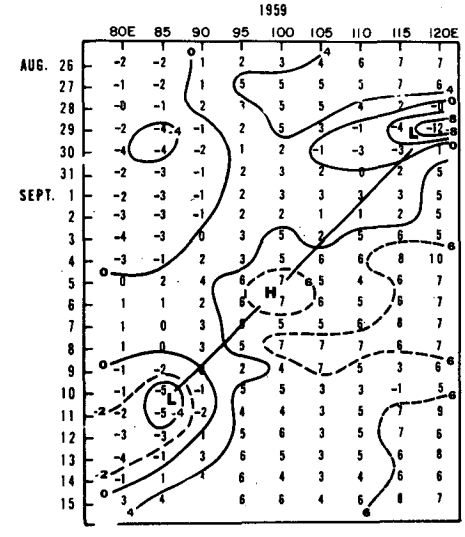

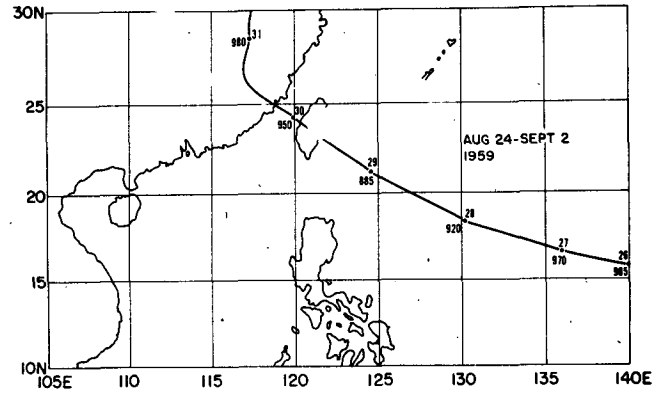

FIG. 4 (*continued*)

(g)

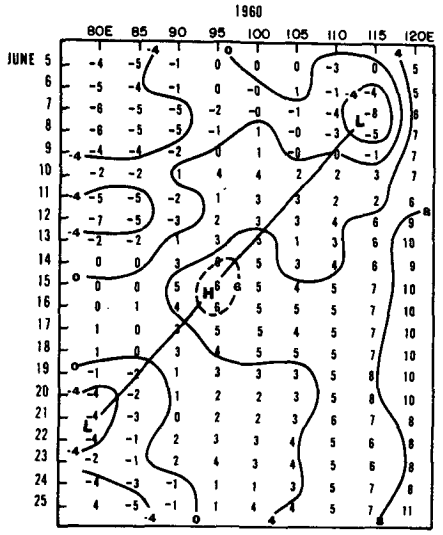

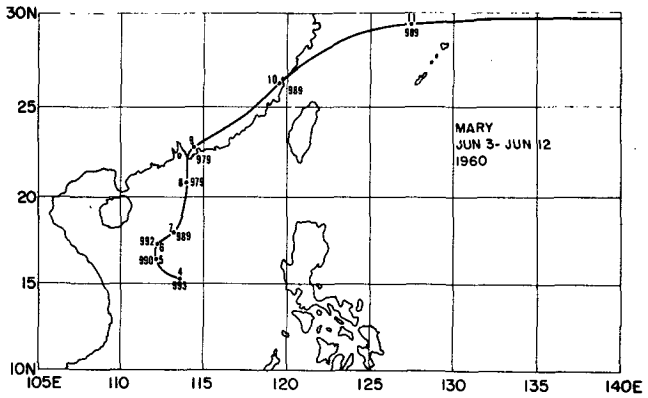

(h)

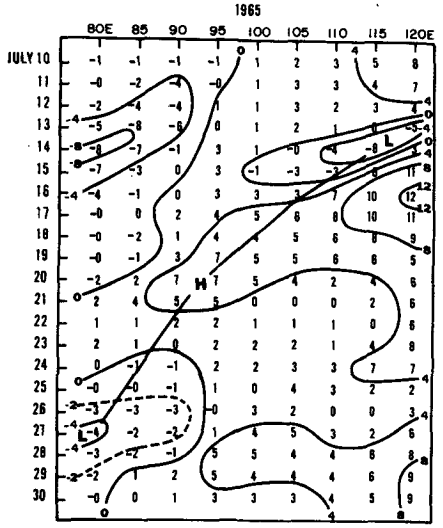

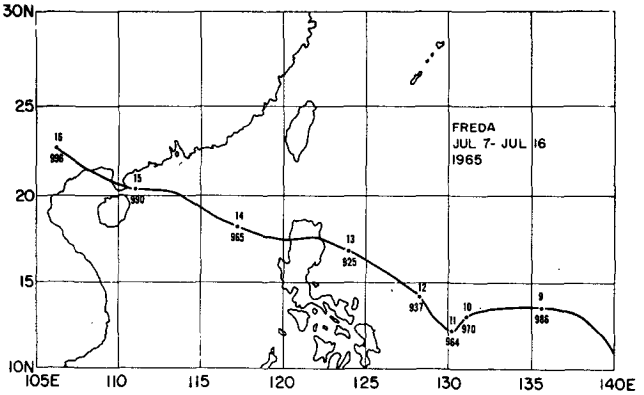

(i)

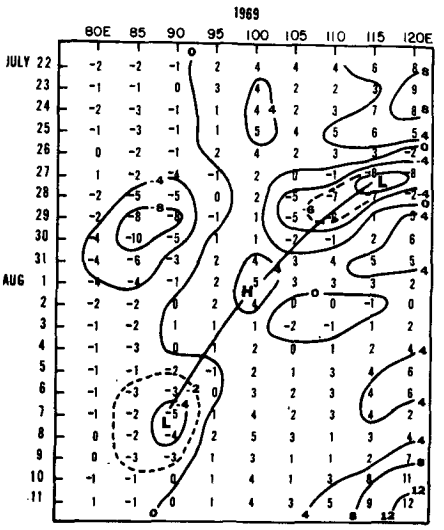

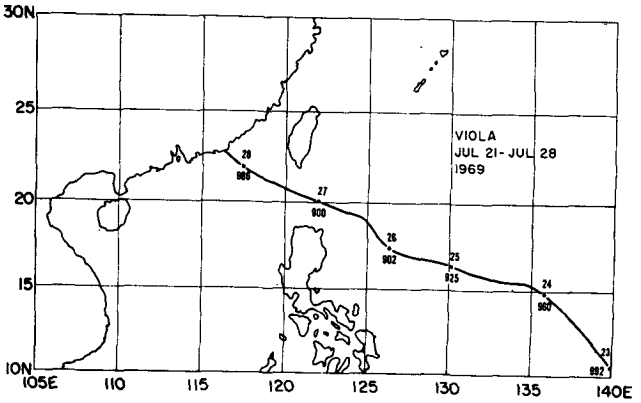

FIG. 4 (*continued*)

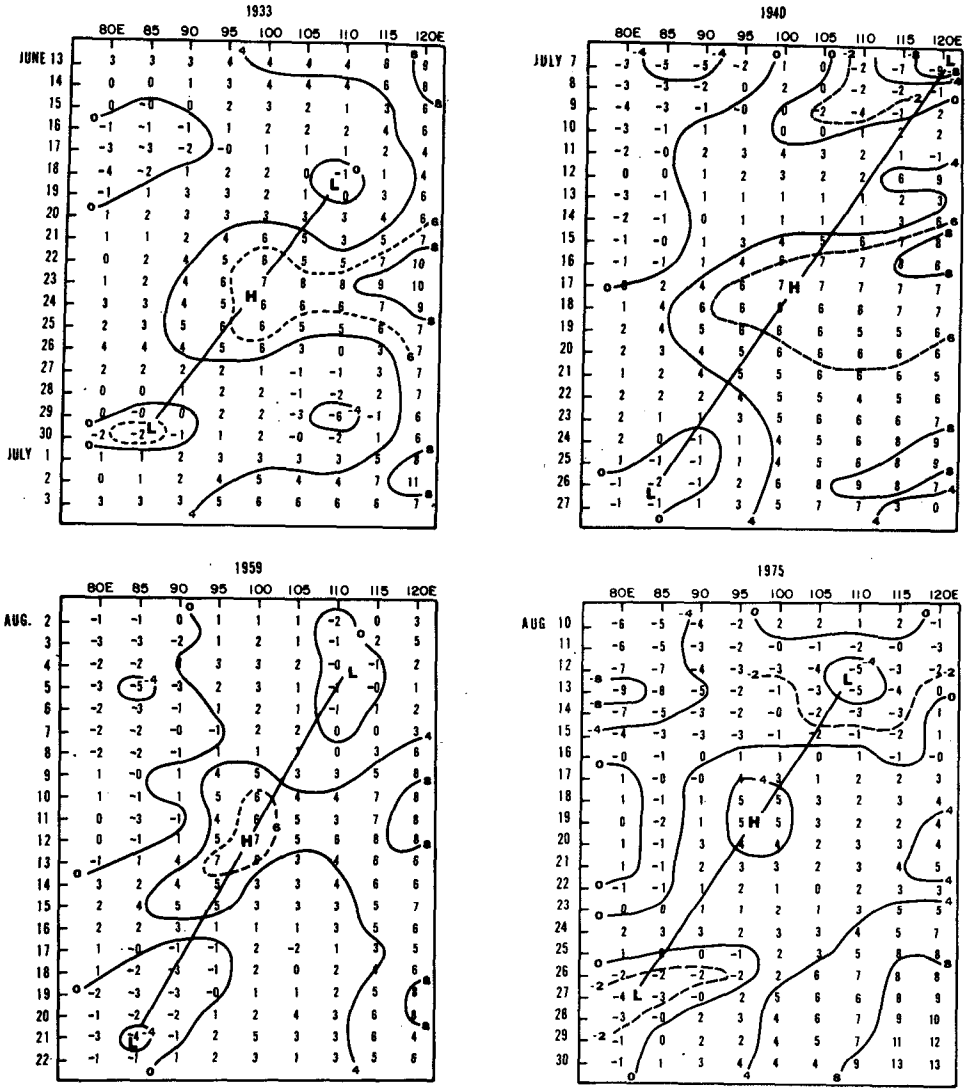

FIG. 5. Additional illustrations of Hovmöller diagrams based on surface pressure data at 20°N. The ordinate shows the date and the abscissa longitude. The surface pressures are departures from 1000 mb.

were isolated for the months of June through early September. The complete set of Hovmöller diagrams and associated typhoon tracks for these examples is given in Krishnamurti *et al.* (1977). Table 1 contains a summary of the events for which tropical cyclone tracks could be found. The speed of westward propagation of the amplification ranges from 1.2° to 3.9° longitude day^{-1}. We may summarize the results of these 23 examples as follows: Roughly a week after the pressure fall occurs over the Asian coast after the typhoon's arrival, a gradual pressure rise of about 5 mb occurs over central Indochina. During the ensuing week a monsoon disturbance forms over the northern part of the Bay of Bengal (or its vicinity). The line connecting the low-high-low sequence is much like the downstream amplification diagrams of middle latitudes with an important distinction. The phase speed of westward propagation of the disturbance is much larger than the speed of propagation of the amplification (i.e., the group velocity). In the following sections we shall discuss this in somewhat further detail. Some additional examples of downstream amplification for which typhoon tracks were not found are shown in Fig. 5. Krishnamurti *et al.* (1977) provide a number of other examples of this type, most of which occurred before 1950. For many of these, we did not have access to typhoon tracks and daily weather charts for each day during the last 45 years. It is our feeling that, around the starting date of the amplification event, a tropical storm was located near the Asian coast for many of these examples. Further analysis of the data may be necessary to determine the possible role of other weaker Pacific disturbances in exciting monsoonal activity.

The sequence of events for tropical downstream

TABLE 1. A summary of 23 of the downstream amplification events. Typhoon names were not available prior to 1952.

Event number	Dates	Storm name	Speed of downstream amplification (deg longitude day^{-1})
1	25 June–15 July 1941	—	2.7
2	16 July–5 Aug 1942	—	2.3
3	17 July–6 Aug 1943	—	1.3
4	12 July–1 Aug 1946	—	3.9
5	8 June–12 June 1948	—	2.5
6	16 June–6 July 1951	—	2.7
7	14 July–13 Aug 1952	Harriet	2.8
8	8 Aug–28 Aug 1953	Ophelia	2.8
9	28 Aug–17 Sept 1954	Ida	1.6
10	14 Aug–3 Sept 1957	—	1.9
11	13 July–2 Aug 1958	Betty	2.5
12	26 Aug–15 Sept 1959	—	2.7
13	5 June–25 June 1960	Mary	2.5
14	14 July–3 Aug 1961	Elsie	2.2
15	19 July–8 Aug 1962	Kate	1.7
16	7 Aug–17 Aug 1963	Carmen	2.8
17	5 Aug–25 Aug 1964	Ida	1.9
18	10 July–30 July 1965	Freda	2.7
19	29 July–18 Aug 1967	Fran	1.2
20	21 July–10 Aug 1968	Nadine	3.1
21	22 July–11 Aug 1969	Viola	2.3
22	20 July–9 Aug 1971	Lucy	1.4
23	10 Aug–30 Aug 1974	Lucy	1.6

amplification is far more geographically fixed than its mid-latitude counterpart. We shall show later that this phenomenon is produced by a superposition of quasi-stationary large-amplitude long waves and smaller scale transient progressive waves. The geographically fixed nature of this phenomenon appears to be related to the long-wave geometry and its variations. Fig. 6 shows the positions at landfall of the tropical cyclones listed in Table 1. Most of these storms reached the Asian coast within the area outlined in this diagram.

It should be noted that because the x-t diagrams of surface pressure show data at 5° longitude increments at a single latitude (20°N), the typhoons often passed between data points or at some time of day other than 0000 GMT. For these reasons, the data may indicate pressures only slightly below 1000 mb even though a typhoon has passed through the region represented by the data point. For the same reasons, the lowest values of surface pressure associated with the monsoon disturbances do not always appear on our diagrams, particularly as the storms move west-northwestward out of the Bay of Bengal, away from 20°N (see Fig. 1).

Williams and van Loon (1976) have discussed some discrepancies between the NCAR surface pressure data set and that for the United Kingdom Meteorological Office. In the region of the present study, they find a difference of less than 0.1 mb year^{-1} in the long-term trend of the summer season means for 1955–69. These errors in the mean pressure, although they may be serious in climate studies, should have no significant effect on the results of this study, which deals with changes of pressure on the order of 10 mb in a few days. Williams and van Loon also found several grid points in the NCAR set with large deviations from nearby station values during certain seasons. None of these grid points are part of the present study.

A synoptic sequence of surface pressure charts for a particular case of downstream amplification is shown in Fig. 7. These maps are given at intervals of 2 days each. For example, Typhoon Freda arrives near the Vietnam coast on 14 July 1965. By 20 July, a surface pressure ridge forms along 95°E. Pressure rises 5–10 mb along 95°E all the way between the equator and 40°N during this 6-day period. A monsoonal disturbance forms over the northern Bay of Bengal on 27 July and moves inland by the 28th. A significant pressure drop may be noted all along 90°E longitude. This example will be discussed in detail in Section 5.

4. A composite downstream amplification diagram

Based on the 43 years of these well-defined sequences of downstream amplification a composite diagram was prepared. The center of reference in this diagram is the anticyclone over central Indochina at its maximum intensity during the passage of this phenomenon. Fig. 8 shows the composite Hovmöller diagram. Because of the differences in the speed of propagation of the individual events and in the intensity and size of the pressure systems, the composite structure shows more of a smoothed field than the individual examples. However, it provides a useful measure of mean speed of westward propagation (2.2° longitude day^{-1}) of the downstream amplification.

In the composite as well as in most individual examples we note a low pressure area over eastern India in the early part of the 21-day period. In general, when

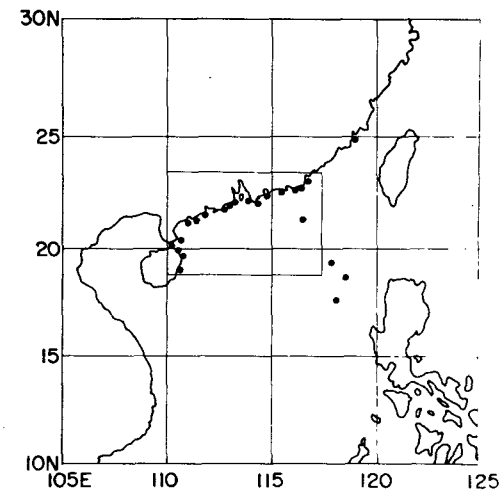

FIG. 6. The location of landfall (or location of recurvature) of typhoons near the Asian coast. These are storms that gave rise to a downstream amplification.

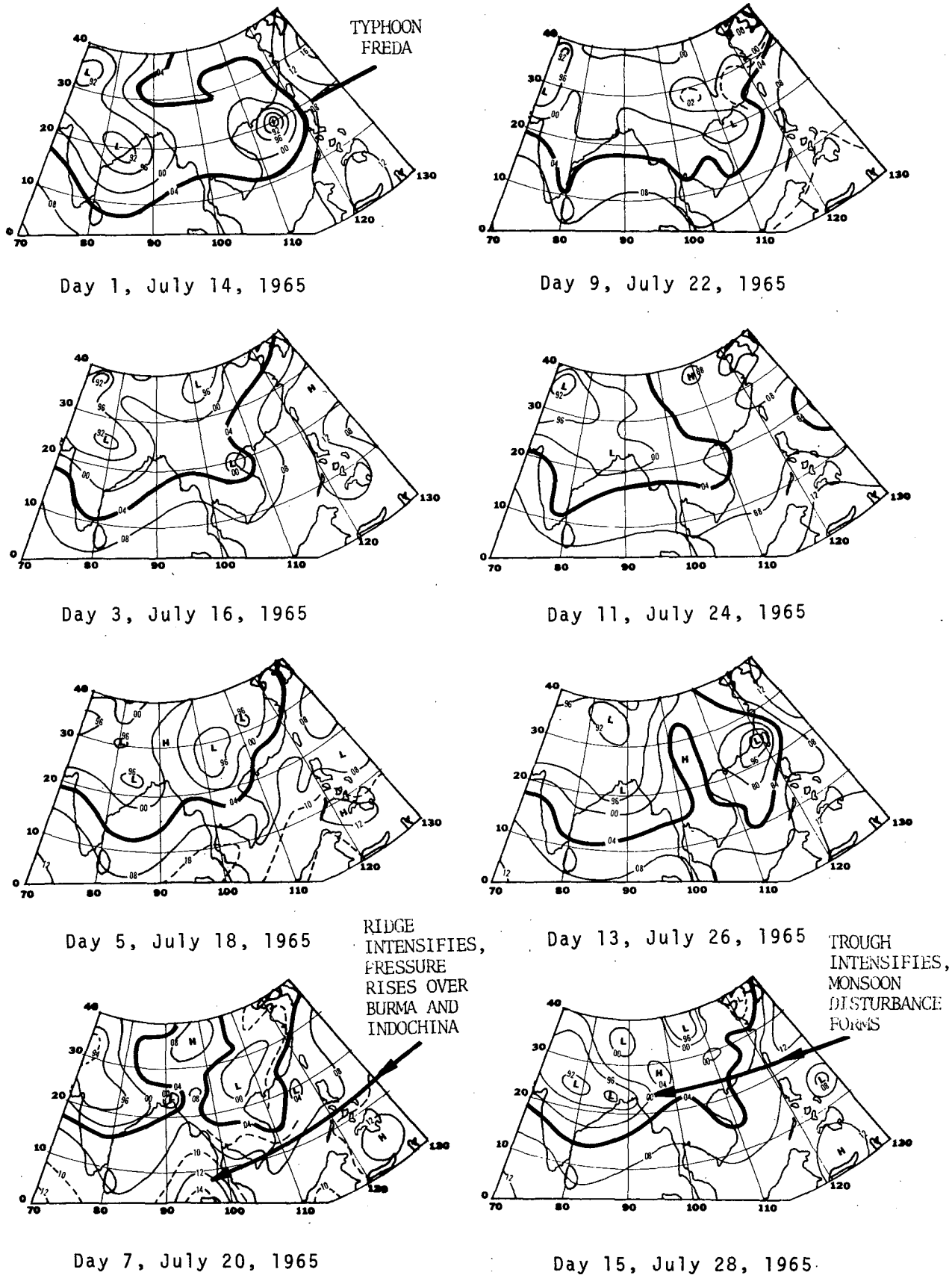

FIG. 7. A synoptic sequence of surface charts (sea level isobars) for a 15-day period at 2-day intervals. The diagram illustrates a downstream amplification event during July 1965. (From Daily Series Synoptic Weather Maps, NOAA.)

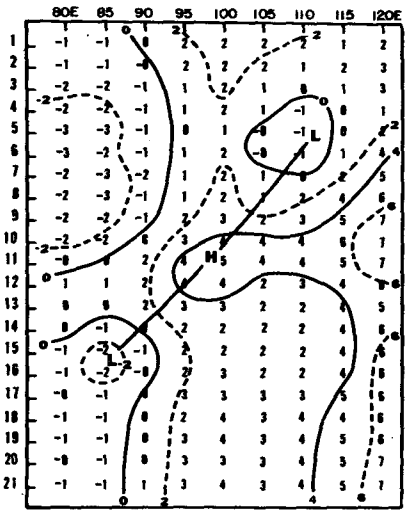

FIG. 8. A composite Hovmöller diagram of the downstream amplification based on 34 individual events. The ordinate is the day number and the abscissa is longitude. Pressure is shown as a departure from 1000 mb.

a typhoon arrives over Indochina, the monsoon trough is usually also fairly intense over eastern India. The typhoon and the monsoon trough contribute to a large variance for zonal wavenumbers 1 and 2 in the zonal harmonics of the surface pressure field. Furthermore, we note that during the course of westward propagation of the amplification, the amplitude of these long planetary waves tends to decrease rapidly for roughly one week and thereafter builds up gradually as the monsoon disturbance forms. The details of the zonal harmonic analysis will be presented in Section 5.

While examining the individual cases we noted that two classes of downstream amplification could be distinguished. The speed of propagation of the amplification is used to distinguish these. Fig. 9 shows two composite diagrams based on the fast (2.5° longitude day^{-1}) and the slow (1.7° longitude day^{-1}) moving cases. As may be seen from these diagrams the intensity of the disturbance in the composite structure of the two categories is somewhat different. As a result the overall composite of all cases (Fig. 8) is not representative of all cases. In any practical application of this notion of downstream amplification, care should be exercised in the use of these composite diagrams.

5. Phase versus group velocity

From zonal harmonic analysis and wave superposition exercises, we noted that wavenumbers 1–12 adequately describe the downstream amplification phenomenon at 20°N. An example of this wave superposition is illustrated in Fig. 10 for July 1965.

a. Long waves

Fig. 10a shows the x-t diagram for the long waves (wavenumbers 1 and 2). This is a quasi-stationary part of the waves that is very important for the amplification phenomenon. These quasi-stationary waves exhibit a decrease in their amplitude during the first week and a gradual buildup of amplitude during the second week. We feel that the typhoon's arrival near the Vietnam coast, the subsequent westward push of the Pacific anticyclone, and the subsequent formation of the monsoon depression over the Bay of Bengal some two weeks later are related to the variation in the amplitude of the long waves.

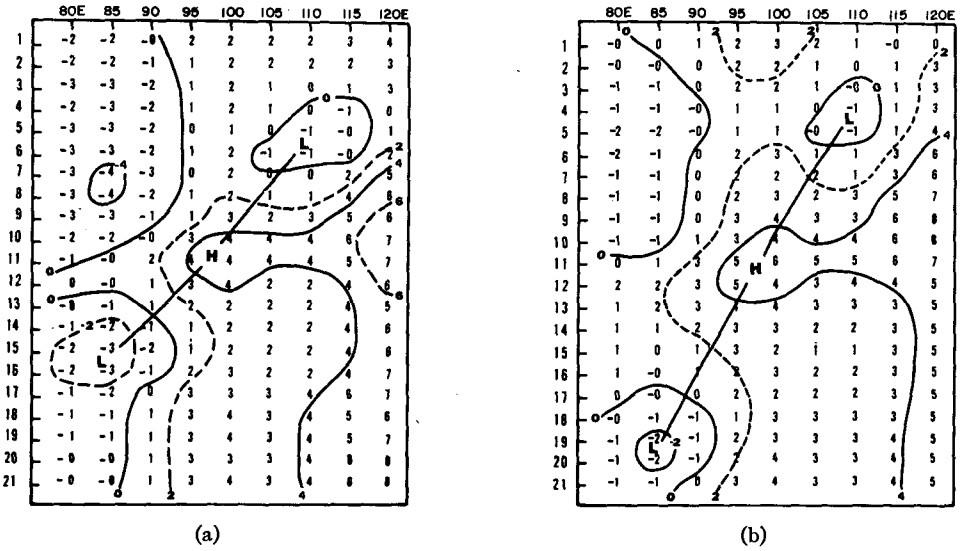

(a) (b)

FIG. 9. A composite Hovmöller diagram based on a subset of cases shown in Fig. 8 where the group velocity is on the order of (a) 2.5° longitude day^{-1} and (b) 1.7° longitude day^{-1}.

b. Short waves

Fig. 10b shows an x-t diagram for the shorter waves (wavenumbers 3–12). These are westward propagating transient waves. As may be noted, these waves travel westward from the western Pacific across into the Indian subcontinent. The amplitude of this wave package is small enough to be masked by the large-amplitude long waves when one examines the entire pressure field (Fig. 4h). The existence of this westward moving package of waves across Indochina is a major finding of the present study. The westward propagation speed of this package is about 8 m s^{-1}.

c. Superposition of waves

Fig. 10c illustrates an x-t diagram for the first 12 waves. This diagram is obtained by adding Figs. 10a and 10b. It may be seen by comparing this sum of the first 12 waves with the total picture for this event shown in Fig. 4h, that the phenomenon of downstream amplification is, in fact, captured by the first 12 zonal harmonics. The observed features of downstream amplification suggest that the phenomenon is not explainable as a simple linear problem. The transient waves (wavenumbers 3–12) do not by themselves exhibit the downstream amplification. The large variation in the

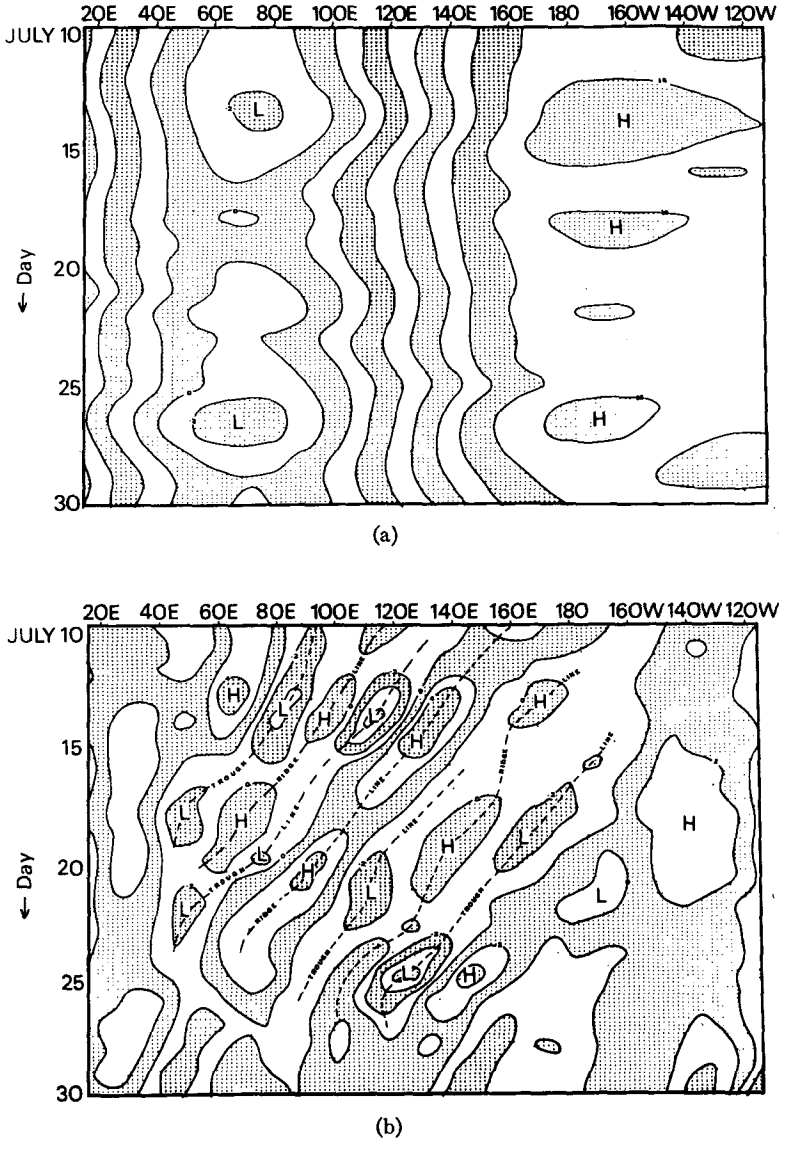

FIG. 10. Hovmöller diagram based on global sea level pressure (mb) data at 20°N during July 1965 for (a) the sum of zonal wavenumbers 1 and 2; (b) the sum of zonal wavenumbers 3–12; and (c) the sum of zonal wavenumbers 1–12. Fig. 10c should be compared to Fig. 4h, which shows the original pressure data.

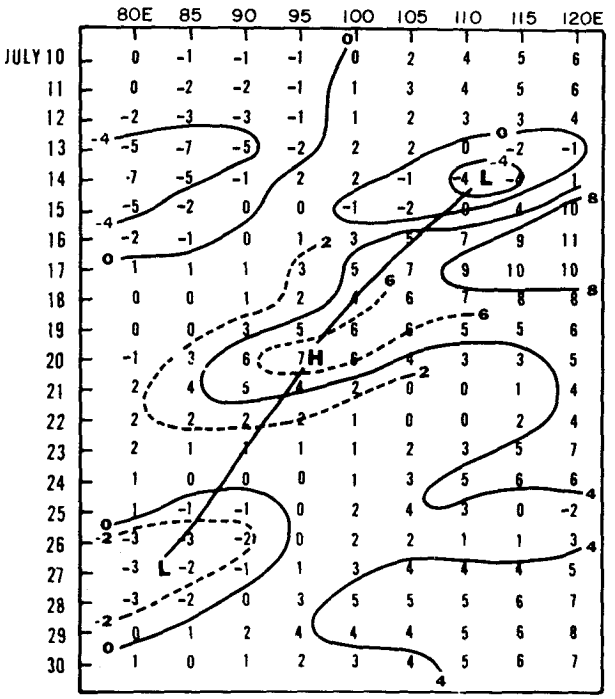

(c)

amplitude of the quasi-stationary long waves plays an important role in the wave superposition and in the realization of the final geometry of the downstream amplification. If the variation in the amplitude of the long waves is averaged out, wave superposition does not produce the observed geometry.

d. Phase versus group velocity

The total picture (including all waves) in the Hovmöller diagram for 1965 shows the following features

Observed phase velocity: -8 m s^{-1}.

Observed group velocity: -3.3 m s^{-1}.

Thus, we note that the group velocity is slower than the phase velocity. This is, in fact, the case over many regions of the tropics. To illustrate this we have prepared (Fig. 11) a diagram of the group velocity

$$c_g = U_0 + \beta L^2/4\pi^2 \tag{1}$$

for an equivalent barotropic atmosphere (vertically integrated U_0 based on July mean data from 1000 to 100 mb) for a wavelength $L = 2000$ km. Tropical waves of this wavelength have been observed by Reed and Recker (1971) over the western Pacific, by Pedgley and Krishnamurti (1976) over West Africa, and by Krishnamurti *et al.* (1975) over the Indian subcontinent. Most

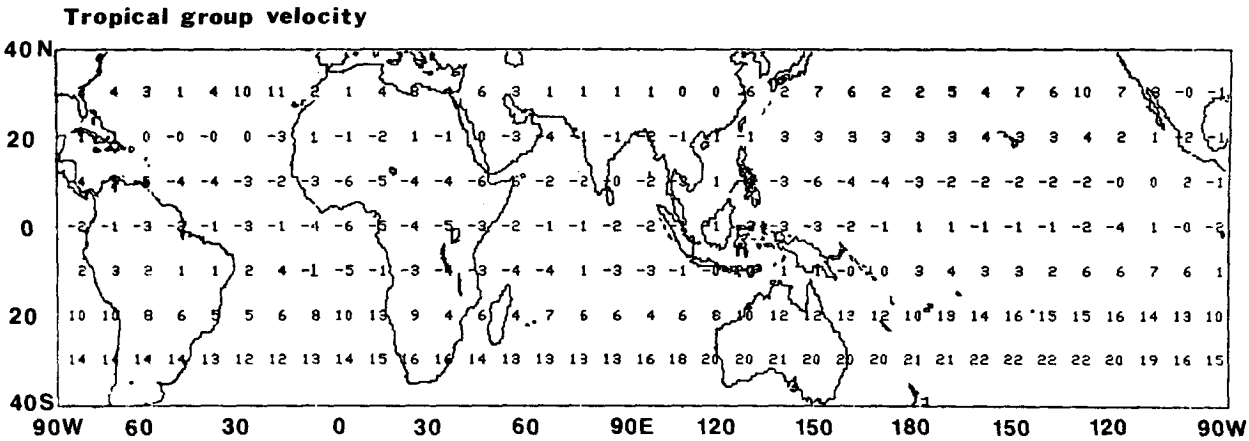

FIG. 11. Distribution of the group velocity $U_0+\beta L^2/4\pi^2$ (m s^{-1}) over a global tropical belt based on July mean, vertically integrated zonal velocity.

of these abovementioned disturbances are known to propagate westward at a speed of roughly 5° to 7° longitude day^{-1}. The local estimate of the group velocity in these regions of tropical disturbances is thus smaller than the phase velocity. This is an important observation that could be exploited for empirical prediction of downstream amplification because of its slow rate of westward propagation over the tropics.

e. The barotropic group velocity on a beta plane

Following Matsuno (1966) and Lindzen (1967), the dispersion relation for free oscillations for two-dimensional barotropic dynamics on a beta plane is (see the Appendix)

$$\omega^3-\left[f_0^2+k^2gh+\left(\frac{2n}{a}\right)^2gh\right]\omega-k\beta gh=0. \qquad (2)$$

The symbols are defined in Table 2. In Eq. (2), $(n-1)$ designates the number of nodes for the meridional velocity profile from equator to pole. For our study, we choose $n=9$, which corresponds to a meridional length scale of 10° latitude, close to the observed scale of the wave. A dispersion diagram showing the relation between the frequency ω and the nondimensional zonal wavenumber s based on Eq. (2) for $n=9$ is illustrated in Fig. 12. Following earlier works by Matsuno (1966) and Lindzen (1967), we have distinguished the slow moving Rossby waves from the gravity waves. Our interest is in the westward moving Rossby waves which are shown in the lower left portion of this diagram where $w/k<0$. It is of interest to note that for the ranges of k we are interested in, i.e., $k=1$–12, westward moving group velocity $(d\omega/dk<0)$ exists for these Rossby waves.

We note that the only effect of including a constant basic zonal current U_0 in the derivation of Eq. (2) (see the Appendix) would be to replace ω by the Doppler-shifted frequency $\omega+kU_0$. We note further that for Rossby waves, $\omega\approx10^{-6}$ s^{-1}, and $f_0^2\omega\gg\omega^3$. Hence ω^3 may be neglected in order to obtain an approximate expression for the group velocity from Eq. (9)[1], i.e.,

$$c_g=U_0+\frac{\beta\left[\frac{4\pi^2}{L^2}-\frac{f_0^2}{gh}-\left(\frac{2n}{a}\right)^2\right]}{\left[\frac{4\pi^2}{L^2}+\frac{f_0^2}{gh}+\left(\frac{2n}{a}\right)^2\right]^2}. \qquad (3)$$

Without the second and third terms in the numerator and the denominator, we have the familiar one-dimensional group velocity for Rossby waves.

Observations show the tropospheric mean value of $U_0\approx-2.7$ m s^{-1} in our region of interest. Because most monsoon disturbances extend to the 300–200 mb layer (Krishnamurti *et al.*, 1975; Murakami, 1976), and because many authors have emphasized the importance of steering by the high-level easterlies, we feel that this computation of an equivalent barotropic group velocity with a tropospheric mean $U_0\approx-2.7$ m s^{-1} is relevant to our problem. From the composite downstream amplification diagram (Fig. 8), we choose a 25° longitude wavelength. Using this wavelength, the group velocity of pure Rossby waves [from Eq. (1)] is -0.3 m s^{-1}. This is quite low compared to the observed mean group velocity (Fig. 8), which is roughly -2.7 m s^{-1}. If we use Eq. (2), and take an equivalent depth $h=10$ km and a meridional scale $n=9$, we find that $c_g\approx-3.0$ m s^{-1}, which is somewhat close to the observed value. We thus conclude that meridional variation, represented by the term $(2n/a)^2$, is important and we are dealing with two-dimensional Rossby waves. A tabulation of the group velocity as a function of wavelength is illustrated in Table 3.

TABLE 2. List of symbols.

Symbol	Meaning
u	zonal velocity
v	meridional velocity
ϕ	geopotential height
h	equivalent depth or mean depth of fluid
f	Coriolis parameter
g	acceleration of gravity
β	beta parameter
U_0	vertical integrated zonal velocity
L	wavelength
c_g	group velocity
ω	frequency
f_0	Coriolis parameter at reference latitude
k	east-west global wavenumber
s	nondimensional wavenumber $[=ka\cos\phi_0]$
ϕ_0	reference latitude
a	radius of the earth
n	wavenumber

TABLE 3. Group velocity (m s^{-1}) as a function of zonal wavenumber.

Nondimensional wavenumber $s=ka\cos\phi_1$	Group velocity c_g No basic current	With basic current
−1	−2.7	−5.4
−2	−2.6	−5.3
−3	−2.5	−5.2
−4	−2.3	−5.0
−5	−2.1	−4.8
−6	−1.9	−4.6
−7	−1.6	−4.3
−8	−1.4	−4.1
−9	−1.2	−3.8
−10	−1.0	−3.7
−11	−0.8	−3.5
−12	−0.6	−3.3
−13	−0.4	−3.1
−14	−0.3	−3.0

[1] Solving the cubic equation directly and then choosing the Rossby wave solution changes the results by less than 0.1%.

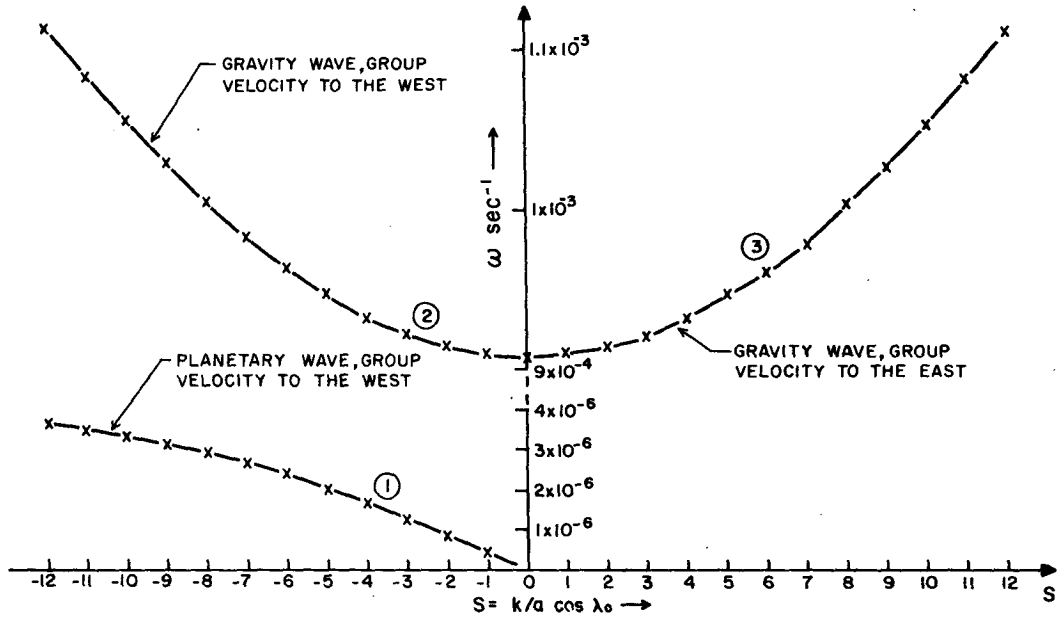

FIG. 12. A dispersion diagram for $n=9$ mode on a beta plane at 20°N. The ordinate is the frequency ω and the abscissa is the real part of the nondimensional wavenumber s.

For reasons stated earlier, the limitations of linear analysis are obvious. The analysis, however, offers an explanation for the downstream amplification phenomenon, that these are most likely Rossby waves with a westward propagating phase velocity which is about three times as large as the westward propagating group velocity. This linear analysis is merely suggestive of the dynamics. We do not feel that it can be of much help in the actual prediction of episodes of downstream amplification since it leaves out the large-amplitude variations of the long waves.

6. Concluding remarks

The principal conclusion of this study is that monsoon disturbances (including depressions) do not always form *in situ* over the northern part of the Bay of Bengal. A substantial number of them form via a downstream intensification mechanism. The mechanism is best illustrated in the so-called Hovmöller diagram, which shows that wave superposition of quasi-stationary long waves and westward traveling shorter waves gives rise to this propagation of amplification. The westward moving disturbances, in fact, come all the way from the western Pacific to the Indian subcontinent. The group velocity of the waves is close to that of middle-latitude Rossby waves at 20°N. The observed phenomenon itself appears to be somewhat more complex than a mere linear wave superposition, since we observe a large oscillation in the broadscale pressure field. Krishnamurti and Bhalme (1976) and Murakami (1976) have noted a quasi biweekly oscillation in many parameters of the broad-scale monsoons. In this study, the oscillation in the amplitude of the long waves (Fig. 10a) indicates this type of behavior very clearly. If we assume that this is a natural oscillation of the broadscale monsoon system, then perhaps we might view the formation of a monsoon disturbance as an interaction of the large-scale, quasi biweekly standing oscillation with westward propagating smaller scale transients. We feel that for a better understanding of the problem, one may have to invoke nonlinear theory.

Although the results presented here are based on an examination of long-term data records (43 years of surface pressure), we feel that a word of caution needs to be expressed on the applicability of the principle expanded here. It is well known that an average of about two monsoon depressions and six monsoon lows form each month during the active monsoon period between June and September. Over 43 years, there are a much larger number of monsoon disturbances than have been discussed here. In this study, however, we have illustrated only a small number of available cases. Krishnamurti *et al.* (1977) display 35 well-defined examples of downstream amplification. In addition, the 43 years of surface pressure data show many more such examples, some of which are not as clearly defined, and many others which occur in succession, such that in a three-week period there is more than one event in the x-t diagram. Although only a small fraction of monsoon lows and depressions are excited by typhoons, and not all typhoons at 20°N near the Asian coast excite a downstream amplification, we believe that the scheme still has application within the following context. If the first half of the x-t diagram, based on observation, appears to resemble the upper half of the Hovmöller diagrams shown in Fig. 4 then one might

make a prediction of the formation of a monsoon disturbance during the ensuing second half-period. We feel that because a large number of examples of downstream amplification have been demonstrated from unsmoothed data, its potential use should be very carefully exploited for predictive purposes.

Further observational studies on the three- and four-dimensional structure of this event are necessary. As a feasible problem one can composite all the upper air observations over the monsoonal belt that define the spectacular individual cases with respect to a center of reference, such as the high over Indochina. The compositing would have to invoke a space-time concept in order to produce a definitive vertical structure for this time-dependent phenomenon. In addition, the various examples of amplification over the northern Bay of Bengal can be classified as to which are monsoon lows, depressions or intensification of the monsoon trough. We hope to present such results in a second part of this study.

There probably are several other tropical regions where the westward propagating group velocity is important in the wave superposition and initiation of tropical disturbances. Global tropical data sets, such as those that will become available from the First GARP Global Experiment during 1979, may be extremely useful for examining other regions where this kind of phenomenon may be prevalent. A cursory examination of satellite photographs suggests that the ITCZ waves in the Pacific do frequently exhibit a downstream amplification. Hence, we feel that there is a potential for further studies along the lines suggested here.

Acknowledgments. The research reported here was supported by the National Science Foundation under Grant ATM 75-18945. The data used in this study were obtained from the National Center for Atmospheric Research, Boulder, Colo. and from the National Climatic Center at Asheville, N. C. Calculations were performed on the CDC 6600/7600 system of the National Center for Atmospheric Research. The National Center for Atmospheric Research is sponsored by the National Science Foundation. The drawings reported here were prepared by Linda Koss and Ellen Laflin.

APPENDIX

Barotropic Group Velocity on a Beta Plane

We shall briefly derive an expression for the group velocity for waves on a beta plane relevant to our study. We start with the familiar linearized barotropic dynamics, discussed by Matsuno (1966). The equations of motion and mass continuity are as follows (see Table 2 for a list of symbols):

$$\frac{\partial u}{\partial t}-fv+\frac{\partial \phi}{\partial x}=0, \tag{A1}$$

$$\frac{\partial v}{\partial t}+fu+\frac{\partial \phi}{\partial y}=0, \tag{A2}$$

$$\frac{\partial \phi}{\partial t}+gh\left(\frac{\partial u}{\partial x}+\frac{\partial v}{\partial y}\right)=0, \tag{A3}$$

where h is the mean depth of the fluid layer. We substitute solutions of the form

$$\begin{Bmatrix} u \\ v \\ \phi \end{Bmatrix}=\begin{Bmatrix} U(y) \\ V(y) \\ \Phi(y) \end{Bmatrix}\exp[i(kx-\omega t)], \tag{A4}$$

in Eqs. (A1)–(A3). Upon elimination of U and Φ in the resulting equations and by using the beta plane approximation, a single meridional mode can be defined by

$$\frac{d^2V}{dy^2}+\left[\frac{\omega^2}{gh}-\frac{(f_0+\beta y)^2}{gh}-k^2-\frac{\beta k}{\omega}\right]V=0. \tag{A5}$$

We next neglect terms where β is multiplied by y but retain it in such terms where it is multiplied by a constant and obtain (here we are introducing the middle-latitude beta plane assumption since the disturbance of interest propagates near 20°N)

$$\frac{d^2V}{dy^2}+\left[\frac{1}{gh}(\omega^2-f_0^2)-k\left(\frac{\beta}{\omega}+k\right)\right]V=0. \tag{A6}$$

We next define $d=a(\pi/2-\phi_0)$, where ϕ_0 is a reference latitude and a the radius of the earth. Let nondimensional wavenumber $S=ka\cos\phi_0$ and $S=0, \pm1, \pm2$ define a cyclic zonal boundary condition. We shall use for the meridional boundary conditions

$$V=\begin{cases} 0, & \text{at } y=+d \quad \text{(i.e., at the North Pole) for } S\neq 1. \\ 0, & \text{at } y=-a\phi_0 \text{ (i.e., at the equator).} \end{cases}$$

The condition at $y=+d$ is based on the behavior of solutions of Laplace's tidal equation and the condition $V=0$ at $y=-a\phi_0$ is an imposed rigid wall boundary condition.

With the above boundary conditions, the solutions of (A6) may be expressed by

$$V=\sin[(2n/a)(d-y)], \tag{A7}$$

$$(1/gh)(\omega^2-f_0^2)-k(\beta/\omega+k)=(2n/a)^2, \tag{A8}$$

where n is an integer.

Eq. (A8) may be rewritten as

$$\omega^3-[f_0^2+k^2gh+(2n/a)^2gh]\omega-k\beta gh=0 \tag{A9}$$

which is equivalent to Eq. (2) in the text.

REFERENCES

Chin, P. C., 1958: *Tropical Cyclones in the Western Pacific and China Sea Area.* Royal Observatory, Hong Kong, 89 pp.

Hovmöller, E., 1949: The trough-and-ridge diagram. *Tellus*, **1**, 62–66.

India Meteorological Department, 1964: *Tracks of Storms and Depressions in the Bay of Bengal and the Arabian Sea*. India Meteorological Dept., New Delhi, 167 pp.

Keshavamurty, R. N., 1971: On the maintenance of the mean monsoon circulation and the structure and energetics of monsoon disturbances. Ph.D. thesis, Mysore University, 192 pp.

Krishnamurti, T. N., and B. J. Higgins, 1967: An investigation of meteorological conditions during a California rainfall period. University of California Water Resources Center, Contrib. No. 119, 70 pp.

——, and H. Bhalme, 1976: Oscillations of a monsoon system. Part I, Observational aspects. *J. Atmos. Sci.*, **33**, 1937–1954.

——, J. Molinari, H. L. Pan and V. Wong, 1977: Downstream amplification and formation of monsoon disturbances. Rep. No. FSU 77-2, Dept. of Meteorology, Florida State University, 52 pp.

——, M. Kanamitsu, R. Godbole, C. B. Chang, F. Carr and J. H. Chow, 1975: Study of a monsoon depression (I), Synoptic structure. *J. Meteor. Soc. Japan*, **53**, 227–240.

Lindzen, R., 1967: Planetary waves on beta planes. *Mon. Wea. Rev.*, **95**, 441–451.

Matsuno, T., 1966: Quasi-geostrophic motions in the equatorial area. *J. Meteor. Soc. Japan*, Ser. II, **44**, 25–43.

Murakami, M., 1976: Analysis of summer monsoon fluctuations over India. *J. Meteor. Soc. Japan*, **54**, 15–31.

National Oceanic and Atmospheric Administration, 1949–1976: Daily Series Synoptic Weather Maps. U. S. Department of Commerce, Washington, D. C.

Parry, H., and C. Roe, 1952: Record low temperatures in the mid-Atlantic and east central states, October 20–22, 1952. *Mon. Wea. Rev.*, **80**, 195–202.

Pedgley, D. E., and T. N. Krishnamurti, 1976: Structure and behavior of a monsoon cyclone over West Africa. *Mon. Wea. Rev.*, **104**, 149–167.

Reed, R. J., and E. E. Recker, 1971: Structure and properties of synoptic-scale wave disturbances in the equatorial western Pacific. *J. Atmos. Sci.*, **28**, 1117–1133.

Staff, Central Meteorological Observatory, 1951: *Trajectories of Tropical Cyclones*. Tokyo, Japan, 49 pp.

Staff, United States Fleet Weather Central, Joint Typhoon Warning Center, Guam, 1960–1975 (16 volumes). *Annual Typhoon Report*, Naval Weather Service/Air Weather Service.

Wallace, J. M., 1970: Time-longitude sections of tropical cloudiness (December 1966–November 1967). ESSA Tech. Rep. NESC 56, U. S. Dept. of Commerce, 37 pp.

Williams, J., and H. van Loon, 1976: An examination of the Northern Hemisphere sea-level pressure data set. *Mon. Wea. Rev.*, **104**, 1354–1361.